
EFDA–JET–CP(03)01-69

S. Brezinsek, P.T. Greenland, A. Pospieszczyk, A. Kirschner, G. Sergienko,
Ph. Mertens, V. Philipps, U. Samm, A. Meigs, M. Stamp
and JET EFDA Contributors*

Spectroscopic Studies of Carbon Sources in Present Tokamaks

Spectroscopic Studies of Carbon Sources in Present Tokamaks

S. Brezinsek¹, P.T. Greenland², A. Pospieszczyk¹, A. Kirschner¹, G. Sergienko¹,
Ph. Mertens¹, V. Philipps¹, U. Samm¹, A. Meigs³, M. Stamp³
and JET EFDA Contributors*

¹*Institut für Plasmaphysik, Forschungszentrum Jülich GmbH, EURATOM-Association
Trilateral Euregio Cluster, D-52425 Jülich, Germany*

²*QOLS, Blackett Laboratory, Imperial College, London SW7 BZ, UK*

³*EURATOM/UKAEA Fusion Association, Culham Science Centre, Oxon OX14 3DB, UK*

**See Annex of J. Pamela et al., "Overview of Recent JET Results and Future Perspectives",
Fusion Energy 2000 (Proc. 18th Int. Conf. Sorrento, 2000), IAEA, Vienna (2001).*

Preprint of Paper to be submitted for publication in Proceedings of the
EPS Conference on Controlled Fusion and Plasma Physics,
(St. Petersburg, Russia, 7-11 July 2003)

“This document is intended for publication in the open literature. It is made available on the understanding that it may not be further circulated and extracts or references may not be published prior to publication of the original when applicable, or without the consent of the Publications Officer, EFDA, Culham Science Centre, Abingdon, Oxon, OX14 3DB, UK.”

“Enquiries about Copyright and reproduction should be addressed to the Publications Officer, EFDA, Culham Science Centre, Abingdon, Oxon, OX14 3DB, UK.”

ABSTRACT.

For the prediction of the lifetime of plasma-facing components made of graphite in future fusion devices, a detailed knowledge about the carbon erosion processes and thus the hydrocarbon particle fluxes is essential [1]. The extrapolation of data from present devices by numerical modeling suffers in particular from large uncertainties about the carbon sources [2]. The formation and release of hydrocarbons is crucial, the quantitative measurement of which is a challenge [3]. Here, we focus on the spectroscopic approach, in which photon fluxes will be converted into particle fluxes by means of inverse photon efficiencies [4]. With this method, the chemical erosion yield Y_{chem} , defined as the ratio of the eroded carbon flux Γ_{C} over the deuterium flux Γ_{D} , has been determined in several experiments. The results show rather strong variations [5], which might, to a large extent, be explained by the use of inadequate inverse photon efficiencies. In this paper we discuss the complexity of the method, in particular based on gas-puff experiments (CD_4 , D_2) for the determination of inverse photon efficiencies performed at JET and TEXTOR.

1. INVERSE PHOTON EFFICIENCIES:

S/XB- and D/XB-values In the case of ionising plasmas, the S/XB-value for species A is the conversion factor between the particle flux Γ_{A} and the photon flux ϕ_{A} [4]

$$\Gamma_{\text{A}} = \frac{4\pi}{Bh\nu} I_{\text{A}} \frac{\langle \sigma_i \nu_e \rangle}{\langle \sigma_e \nu_e \rangle} = \phi_{\text{A}} \frac{S}{\text{XB}} : \quad (1)$$

thereby S stands for ionisation rate, X for excitation rate, B for Branching ratio. In analogy to this we have D/XB-values for molecules where D represents the corresponding Decay rate given by dissociation and ionisation [4]. For an accurate flux determination it is important that no particles escape from the observation volume and that all photons from the electronic transition are detected. When a larger spectral range has to be observed, as it is the case with molecular band emission, it is of particular importance to assure a complete detection of all photons of an electronic transition. Additionally, under realistic experimental conditions we have to take into account several complex phenomena influencing the inverse photon efficiencies.

Experiments in TEXTOR have shown that in the case of the deuterium flux calculation, the molecular source has to be taken into account. A correction term to the S/XB-value which depends on surface and plasma conditions and which can be as large as the original S/XB-value [6] has to be included. However, this correction of the S/XB-value for D_{α} is often not included or only empirically taken as a constant. Its variation can be one reason for uncertainties in Y_{chem} . Moreover, the second contribution to Y_{chem} , the hydro-carbon flux is much more difficult to deal with and to determine. If we focus on CD_4 as the main source only, then in the visible range only the light emission from the break-up product CD and not from CD_4 can be observed directly by passive spectroscopy

$$\left[\frac{S}{\text{XB}} \right]_{\text{A}^2\Delta \rightarrow \text{X}^2\Pi}^{\text{CD}_4 \rightarrow \text{CD}} (n_e, T_e) = \frac{\Gamma_{\text{CD}_4}}{\phi_{\text{A}^2\Delta \rightarrow \text{X}^2\Pi}^{\text{CD}_4 \rightarrow \text{CD}} (n_e, T_e)} . \quad (2)$$

By knowing the catabolism of the CD_4 molecule quantitatively the photon efficiency based on the CD-light only implicitly includes the release of all CD_4 . However, in addition to CD_4 also other hydrocarbons C_xD_y are formed, they may contribute to the CD light emission when CD radicals appear along their dissociation chain.

2. EXPERIMENTAL RESULTS AND DISCUSSION – THE CD RADICAL

We performed CD_4 gas-puff experiments at JET to study the dependence of the resulting CD photon flux and finally of the inverse photon efficiency for CD_4 on the plasma parameters and the gas injection location. In several discharges CD_4 was introduced into the divertor at a constant rate of ($2 \times 10^{21} \text{ s}^{-1}$) through different Gas Injection Modules (GIM). Here, we concentrate on GIM9, located at the bottom plate of the outer divertor and toroidally circumferential, to provide a homogenous injection into the private ux region (fig.1(a)). To distinguish between intrinsic and injected particles, we performed reference discharges with D_2 injection through GIM10 (outer divertor, vertical plate) to achieve similar local plasma conditions. Additionally to the gas-puff, a sweep of the strike-point from the horizontal target (*ht*) to the vertical target (*vt*) plate was made (fig.1(a)). The spectrum of the $\text{A}^2 \rightarrow \text{X}^2\Pi$ transition of CD was recorded by means of a spectrometer system in Czerny-Turner arrangement ($f=1 \text{ m}$, dispersion 0.018 nm/pixel , wavelength coverage 13.5 nm) in a direct view of the outer divertor. A part of the spectrum and its simulation are depicted in figure 1(b). Due to the overlap of lines from O, D, and Be with the P-branches of the A-X transition of CD usually only the strongest part of the spectrum, the spectral region between 429.4nm and 430.9nm which covers mainly the Q-branches of the two strongest vibrational transitions, is used as the standard signal for CD [8]. But also other CD emission ranges are used, which has to be taken into account when comparing CD photon fluxes directly. A spectrum simulation program was developed [7] and the best-fitted spectrum was determined by means of a least-square-fit routine matching the rotational and vibrational population. Simulations for a variety of plasma parameters have shown that only 30% to 50% of the emission from the whole electronic transition is included in the standard spectral range [7]. Without correction for this, the total uxes would be underestimated. The spectrum simulation allows to determine the total photon flux ϕ_{CD} of the A-X transition.

Figure 1(c) shows the spatially and temporally resolved evolution of the CD intensity ICD for a gas injection case and sweeping of the strike-point. ICD is corrected for the background signal from intrinsic hydrocarbons. The negative values in the pre-puff phase (11s-15s) can be referred to a small mismatch of T_e and thus of the intrinsic CD light. ICD increases strongly during the CD_4 gas-puff phase. An expansion of the emission volume is observed and a change of the spatial distribution of light emission is observed with sweeping the strike-point position from *ht* to *vt*. This move of the strike-point is also connected to a change of plasma parameters. Integration of the CD light over all channels gives the total intensity $I_{\text{CD}}^{\text{tot}}$, the time evolution of which is depicted in fig.1d. It shows a strong variation during the strike-point sweep. Surprisingly, even with gas-puff practically no signal can be detected between 15s and 17s, when the strike-point remains unchanged

on the ht plate. During the sweep on the ht plate (17.0s–18.7s), I_{CD}^{tot} increases strongly and then changes only little during the sweep over the vt plate (19.5s–24.0s). When we assume that all CD photons are emitted within the radial extension of the observation volume, then I_{CD}^{tot} is directly proportional to ϕ_{CD} and can be used to derive a D/XB value. But we have to be aware that the line-of-sight does not cover the corner region of the divertor, therefore some photons cannot be detected and the inverse photon efficiencies represent an upper limit. As the gas injection rate is constant, the resulting D/XB-value decreases as long as the strike point sweeps over the ht and reaches a constant value of about 100 when laying on the vt plate. The strike-point position within geometry and plasma parameters are critical points in the determination of ϕ_{CD} and thus of D/XB values for CD4. The determination of ϕ_{CD} can be further complicated as is shown with D2 gas-puff experiments in TEXTOR (fig. 2). A strong overlay of lines of several vibrational bands of the $3D^1\Pi \rightarrow 2P^1\Sigma$ transition of D2 with the A-X transition of CD has been observed. The strongest overlap exists in the standard range of CD and can lead to an overestimation of ϕ_{CD} [7]. Whether this is also the case for JET is still under investigation.

3. INTRINSIC HYDROCARBON FLUX

The determination of Γ_{CD_4} is in the case of intrinsic hydrocarbon sources more complicated. Other hydrocarbons than CD_4 may also contribute to the emission of CD photons after their catabolism. The total photon flux ϕ_{CD} is then given by

$$\phi_{CD} = \phi_{A^2\Delta \rightarrow X^2\Pi}^{CD} = \phi_{A^2\Delta \rightarrow X^2\Pi}^{CD_4 \rightarrow CD} + \phi_{A^2\Delta \rightarrow X^2\Pi}^{C_2D_y \rightarrow CD} + \dots \quad (3)$$

and cannot directly be transferred into CD_4 . However, the total chemical carbon erosion is determined by the sum of all hydrocarbon sources. Especially C_2D_y particles, which can be measured by detecting the C_2 Swan-band [4], contribute also to the total chemically eroded carbon particle flux C. Therefore in the intrinsic case, one has to take into account the contributions from C_2D_y to both radicals, C_2 (Swan band) and CD (A-X).

$$\begin{aligned} \Gamma_C = \Gamma_{CD_4} + 2\Gamma_{C_2D_y} = & \phi_{A^2\Delta \rightarrow X^2\Pi}^{CD_4 \rightarrow CD} \left[\frac{D}{XB} \right]_{A^2\Delta \rightarrow X^2\Pi}^{CD_4 \rightarrow CD} + 2\phi_{A^3\Pi_g \rightarrow X^3\Pi_u}^{C_2D_y \rightarrow C_2} \left[\frac{D}{XB} \right]_{A^3\Pi_g \rightarrow X^3\Pi_u}^{C_2D_y \rightarrow C_2} \\ & + \phi_{A^3\Pi_g \rightarrow X^3\Pi_u}^{C_2D_y \rightarrow C_2} \frac{\left[\frac{D}{XB} \right]_{A^3\Pi_g \rightarrow X^3\Pi_u}^{C_2D_y \rightarrow C_2} \left[\frac{D}{XB} \right]_{A^2\Delta \rightarrow X^2\Pi}^{CD_4 \rightarrow CD}}{\left[\frac{D}{XB} \right]_{A^3\Pi_g \rightarrow X^3\Pi_u}^{C_2D_y \rightarrow CD}} \end{aligned} \quad (4)$$

Figure 3 shows an example from the previously described experiments at JET, where the emission of the C_2 Swan-band becomes very strong during the strike-point sweep over the corner of the inner divertor. In some cases, e.g. at high density plasmas in JET, the formation of C_2D_y can dominate C and thus the chemical erosion [9].

SUMMARY AND CONCLUSION

The spectroscopy of the CD radical is a standard tool in tokamaks for the determination of chemically released hydrocarbon fluxes and the corresponding erosion yields. However, the data published so far at the basis of this method show significant inconsistencies. This is caused to a large extent by incomplete accounting for all relevant effects influencing the inverse photon efficiency. The main effects can be divided into two groups:

- a) Uncertainties in the determination of the total CD photon flux of the A-X transition. Fittings of spectra from the JET divertor have shown that in the CD standard range only 30% to 50% of the total ϕ_{CD} is measured. Ignoring this may lead to an overestimation of the inverse photon efficiencies of up to a factor of 3.
- b) Modification of the inverse photon efficiency due to the presence of various carbon sources. Because of the indirect conversion, which includes the catabolism of the CD₄ molecule, also other hydrocarbons can contribute to ϕ_{CD} after their destruction. This leads to a geometry/surface dependence and thus to modified D/XB-values.

The understanding of inverse photon efficiencies related to the determination of carbon fluxes on tokamaks is progressing. We conclude that for a better interpretation of spectroscopic data, a common data base for inverse photon efficiencies (D/XB-values) is needed (and that older data should be revisited). However, the method shows also certain limitations for a situation with too complex geometries and strongly mixed particle sources. An improved theoretical modeling of erosion-deposition and radiation for a given geometry and plasma background is required for an accurate comparison of experimental data from different tokamaks.

REFERENCES

- [1]. Federici G 2001 Nucl. Fusion **41** No. 12R
- [2]. Kirschner A 2000 Nucl. Fusion **40** 989
- [3]. Philipps V 2000 Nucl. Fusion **40** B293
- [4]. Pospieszczyk A 1993 Controlled Thermonuclear Fusion (Amsterdam: Elsevier Science)
- [5]. Roth J 1999 J. Nucl. Mat. **266-269** 51
- [6]. Mertens Ph 2001 Plasma Phys. Control. Fusion **43** 1
- [7]. Brezinsek S 2003 to be published in Plasma Phys. Control. Fusion
- [8]. Behringer K 1990 J. Nucl. Mat. **176-177** 606
- [9]. Stamp M F 2001 J. Nucl. Mat. **290-293** 321

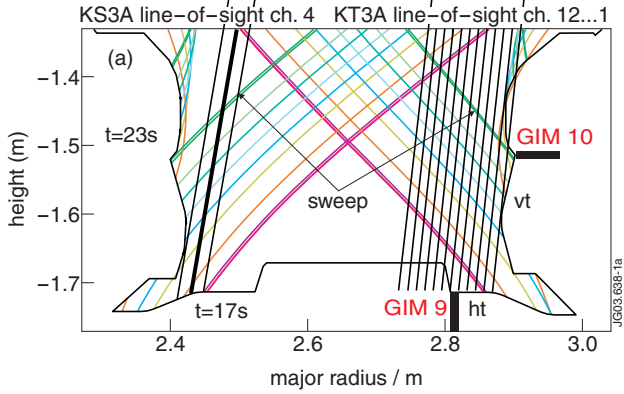


Fig.1(a): Sketch of the JET divertor with the two observation systems marked.

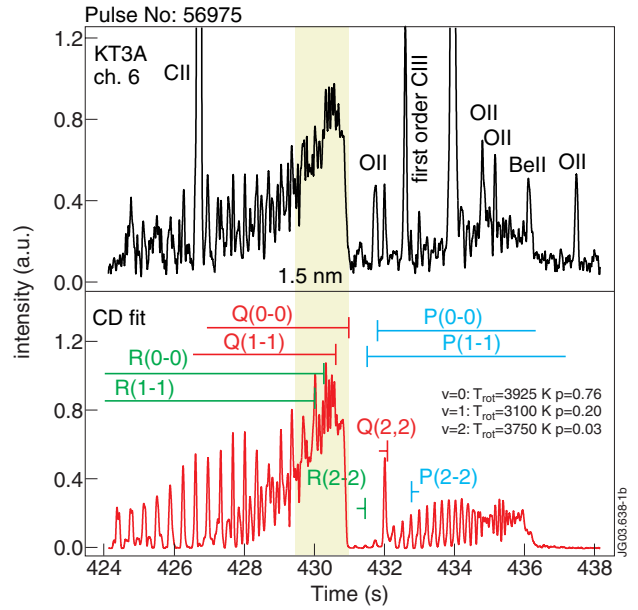


Fig.1(b): Spectra of the A-X transition of CD.

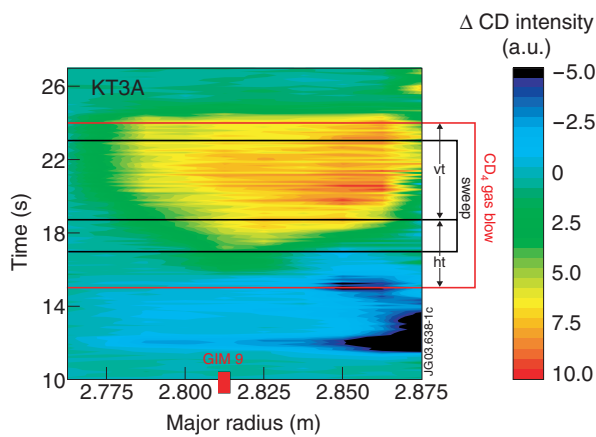


Fig.1(c): Evolution of the CD intensity as function of the major radius during the CD₄ gas injection.

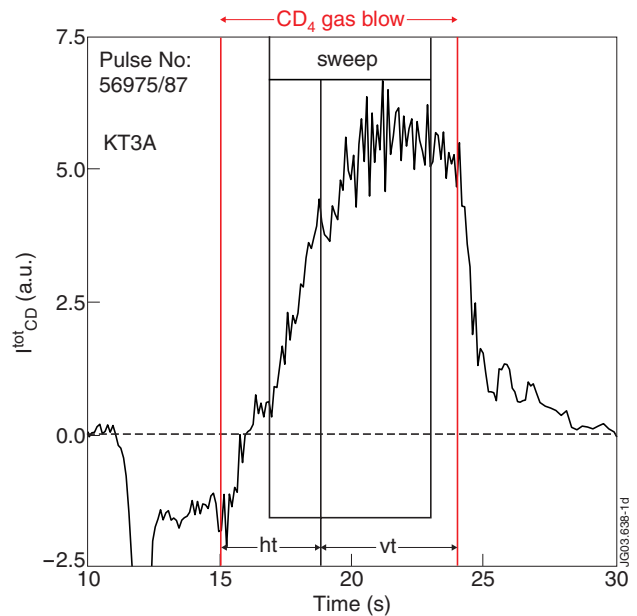


Fig.1(d): Time evolution of the total CD intensity.

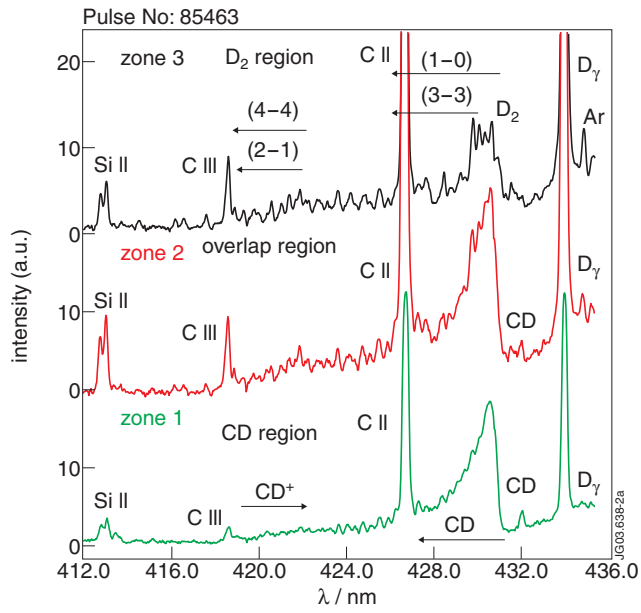


Figure 2: TEXTOR: Strong overlap of D₂ and CD lines during a D₂ gas blow.

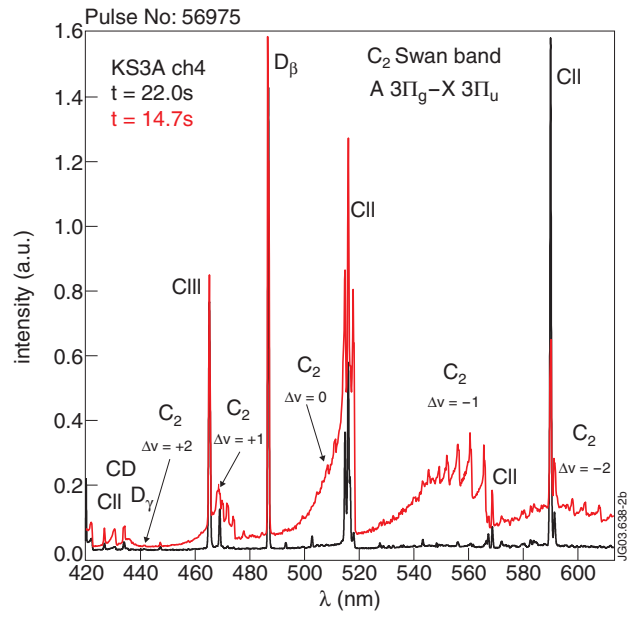


Figure 3: JET: Strong emission of C₂ in the corner region of the inner divertor.